Electrospray Ionization MS of High M.W. TAG Oligomers

W. Craig Byrdwell[a],* and William E. Neff[b]

[a]Florida Atlantic University, Department of Chemistry and Biochemistry, Boca Raton, Florida 33431, and [b]Food and Industrial Oil Research Unit, National Center for Agricultural Utilization Research, ARS, USDA, Peoria, Illinois 61604

ABSTRACT: Reported are the on-line LC/electrospray ionization MS of large, high M.W. oligomers formed from heated triolein, a TAG used as a model for dietary oils. Triolein, the major component of olive oil, canola oil, and other dietary oils, was heated at frying temperature, and the TAG oxidation products were separated using RP-HPLC coupled to an ion trap mass spectrometer *via* an electrospray ionization interface. Ammonium formate was added as a sheath liquid to promote ammonium adduct formation. Masses corresponding to ammonium adducts of intact carbon-linked dimers (*m/z* 1783–1787), trimers (*m/z* 2666–2672), and tetramers (*m/z* 3547–3557) of triolein, with and without additional sites of unsaturation, were observed. Also, dimers, trimers, and tetramers containing one, two, or three additional oxygens, also with and without additional sites of unsaturation, are reported. Based on the formation of some types of triolein dimers, we believe that tristearin might also form dimers, even though it has no readily oxidizable sites of unsaturation. Oxidized tristearin monomers, tristearin dimers, chain-addition products, and chain-shortened products are observed.

Paper no. J10594 in *JAOCS 81,* 13–26 (January 2004).

KEY WORDS: TAG oligomers, TAG oxidation products, triacylglycerols, triglycerides.

The reactions of atmospheric oxygen with fatty acyl chains to form lipid oxidation products have been studied extensively. Many reviews, book chapters, and books dedicated to lipid oxidation products have been published. One excellent reference describing the various aspects of lipid oxidation at ambient temperature was edited by Chan (1). Frankel has published extensively in the area of lipid oxidation, including thorough review articles (2,3). Studies on the oxidation of model FAME such as methyl oleate and methyl linoleate have long shown that oxidation of lipids initially produces hydroperoxides as the primary oxidation products, and these react further to produce a wide array of secondary products. Early work on the mechanisms and products of oxidation was performed on FA and their methyl esters because these were amenable to GC and GC/MS. Analysis of the FAME of oxidation products was also conducted using direct-exposure probe MS, NMR spectrometry, and others (such as IR spectrometry).

At least three broad categories of lipid oxidation products are produced by oxidation of FAME: (i) small volatile oxidation products, (ii) FA fragments, and (iii) dimers, trimers, and other oligomers. The small volatile molecules produced by the breakdown of hydroperoxides have been thoroughly discussed by Frankel (2), Grosch (4), and others. The small volatile oxidation products include alkanes, alkenes, alcohols, aldehydes, ketones, acids, and others. When a small volatile fragment breaks off from the fatty chain, a FA fragment is left behind as a "core aldehyde" or similar residue. The third type of oxidation product, oligomers, are formed when two fatty chains become linked at a site of oxidation. Several classes of dimers of methyl linoleate hydroperoxides were discussed by Miyashita and co-workers (5–7). These were identified by gel permeation chromatography followed by solid-phase extraction and then field desorption MS of derivatized and underivatized products.

The volatile and nonvolatile oxidation products formed from intact TAG also have been studied extensively. The small volatile oxidation products that break off a TAG are amenable to GC/MS, just like the volatiles produced from simple FA. The large intact TAG oxidation products (TAGOX) are not volatile, and so LC has been used for their separation. Mono-, bis-, and tris-hydroperoxides of TAG have been studied by Frankel, Neff, Miyashita, and co-workers (8–10). Hydroperoxides were saponified, transmethylated, and derivatized to their trimethylsilyl ethers (OTMS) and then analyzed using GC and GC/MS. The intact TAG hydroperoxides were analyzed using HPLC with refractive index (RI) or UV detection. The positional distribution of the hydroperoxide groups was determined by lipase hydrolysis. None of these methods, though, constituted the direct on-line HPLC/MS analysis of TAGOX.

High M.W. (HMW) TAGOX are produced by the joining together of intact monomeric TAGOX in a manner analogous to the FA oligomers mentioned above. Since these are large, nonvolatile molecules, they are not amenable to GC or GC/MS analysis. Hopia (11–13) and Marquez-Ruiz (14,15) and co-workers and others have employed size exclusion chromatography (SEC) for their separation and identification. Oligomeric components were detected using RI or ELSD. Although these 2-D detectors provide a quantitative estimate of the total amount of oligomers formed, they do not provide any information about the specific structures of the numerous possible classes of HMW TAGOX possible within a relatively narrow M.W. range (the basis of separation by SEC).

Neff and Byrdwell (16) reported the use of HPLC with atmospheric pressure chemical ionization (APCI) MS of monomeric TAGOX produced from the autoxidation of model TAG, and then from autoxidation of normal and genetically modified canola varieties (17). They then reported the products of heated oxidation at frying temperatures of triolein

---

*To whom correspondence should be addressed at Florida Atlantic University, Department of Chemistry and Biochemistry, 777 Glades Rd., Boca Raton, FL 33431. E-mail: byrdwell@fau.edu

(18). In this report, they showed APCI–MS mass spectra of triolein dimers, formed by joining together two triolein molecules, with and without additional sites of unsaturation and/or oxygen atoms. This represented the first direct HPLC/APCI–MS evidence of on-line separation and identification of HMW TAGOX. The HMW TAGOX were observed in samples in which the oxidized and unoxidized dimers had been enriched by collecting fractions from preparative RP-HPLC. More recently, Byrdwell and Neff (19) showed the first direct identification and characterization of HMW TAGOX with and without additional sites of unsaturation and/or oxygen atoms using electrospray ionization (ESI)–MS. The authors employed a "dual parallel mass spectrometer" arrangement in which both APCI–MS and ESI–MS were performed simultaneously, in parallel, for analysis of monomeric and HMW TAGOX. It was found that without prior enrichment of the HMW TAGOX, APCI–MS was not sufficiently sensitive to identify the HMW TAGOX. However, ESI–MS with ammonium formate added as a sheath liquid allowed facile identification of multiple classes of HMW TAGOX dimers and chain-addition products.

Because ESI–MS was capable of direct identification and characterization of HMW TAGOX, without sample enrichment, this technique has been used in the present report. Here is reported the first use of HPLC/ESI–MS for identification of HMW TAGOX oligomers formed from triolein, including dimers, trimers, and tetramers with and without additional sites of unsaturation and with and without additional oxygen functional groups. We suspect that some dimer formation occurred in a manner that did not involve functional groups down on the fatty acyl chains because we observed dimer formation between two triolein molecules without additional sites of unsaturation or additional oxygen atoms. If this were the case, we concluded that tristearin, which contains only saturated fatty chains, might also be capable of dimer formation. Here, the chromatographic separation and identification of dimers formed by two tristearin molecules, by HPLC/ESI–MS, are reported.

EXPERIMENTAL PROCEDURES

Heated oxidation was performed as previously described (17). Briefly, 5 g of synthetic triolein or tristearin (Nu-Chek-Prep, Elysian, MN) was placed in a 12.5 × 2.0 cm test tube and heated to 190°C by submersion in a temperature-controlled silicone oil bath for 6 h. Samples were dissolved in dichloromethane, transferred to tared vials, and known weights determined. To the heated triolein samples, synthetic trilaurin (C12:0-C12:0-C12:0) and synthetic tristearin were added as internal standards. These internal standards were added to allow us to quantify the relative amounts of the full range of oxidation products formed, to be reported elsewhere. RP-HPLC was performed using an LDC 4100 quaternary pump (Thermo Separation Products; Thermo Finningan, San Jose, CA) with a membrane degasser. Two Inertsil ODS-3 columns in series, 25 cm × 4.6 mm, 5 µm (MetaChem Technologies, Lake Forest, CA) were used. The solvent system used was composed of acetonitrile (ACN) and dichloromethane (DCM). The gradient program was DCM/ACN (30:70, vol/vol) held for 5 min; linear to DCM/ACN (65:35, vol/vol) at 50 min; linear to DCM/ACN (75:25, vol/vol) at 65 min, held to 85 min; recycled to initial conditions at 95 min. A sample volume of 20 µL was injected.

The mass spectrometer was a Finnigan MAT LCQ Deca (Thermo Finnigan). The capillary was operated at 250°C, and the electrospray voltage was set to 5.5 kV. High-purity nitrogen was used as the sheath and auxiliary gases, which were set to 40 and 5 (arbitrary units), respectively. A 20 mM ammonium formate solution in H_2O/ACN (1:4, vol/vol) was added as a sheath liquid from an AB 140B syringe pump (Applied Biosystems, Foster City, CA) at a flow rate of 30 µL/min. Scans were obtained from *m/z* 100–1200 up to 55 min, and *m/z* 500–3700 thereafter. All scans were obtained in centroided positive ion mode. Data-dependent MS/MS (MS^2) and MS/MS/MS (MS^3) were performed, using the most abundant precursor ion from the previous scan. MS^2 and MS^3 were performed using 45% normalized collision energy at a "q" of 0.25. The activation time was 900 ms. MS^n in low-mass mode used an isolation width of 1.5, whereas in high-mass mode the isolation width was 2.0. The ion trap mass spectrometer provided unit resolution with mass accuracy and reproducibility to ~ ±0.1 *m/z* (with ideal calibration) in low-mass mode, up to *m/z* 2000. In high-mass mode, up to *m/z* 4000, some mass accuracy and reproducibility were sacrificed to enable acquisition of higher masses.

RESULTS AND DISCUSSION

Carbon-linked dimers. Figure 1 shows the total ion chromatogram (TIC) of all MS, MS/MS, and MS^3 scans (Fig. 1A), and the TIC of scans obtained in full-scan mode (Fig. 1B). These chromatograms are similar to those that we have reported before (19), showing the presence of numerous monomeric triolein oxidation products. The early-eluting molecules contained one oxidized triolein chain and one or more oxygen functional groups. The extracted ion chromatogram (EIC) at *m/z* 902.8, shown in Figure 1C, showed that the triolein ammonium adduct eluted from 44.5 to 46.5 min ($[OOO + NH_4]^+ = C_{57}H_{104}O_6 + NH_4 = [(57 \times 12.000000 + 104 \times 1.007825 + 6 \times 15.9994) + (14.003074 + (4 \times 1.007825)] = 884.78 + 18.03 = 902.8$, calculated from a table of isotopic weights). The peak in Figure 1D shows the mass range of ammoniated triolein dimers with no additional oxygen functional groups. Two parts of the peak were observed. In the first part of the peak, the *m/z* values were primarily 1783.5/1784.5, whereas in the second half of the peak the *m/z* values were primarily 1785.5/1786.5. The *m/z* values 1785.5/1786.5 corresponded to the ammonium adduct of the dimer formed by two triolein molecules that joined together by losing two hydrogen atoms ($2 \times OOO - 2\ H + NH_4 = 2 \times 884.78 - 2.0 + 18.0 = 1785.6$). A mass spectrum of the second part of this chromatographic peak, from 65.1 to 66.4 min, is shown in Figure 2B, with an

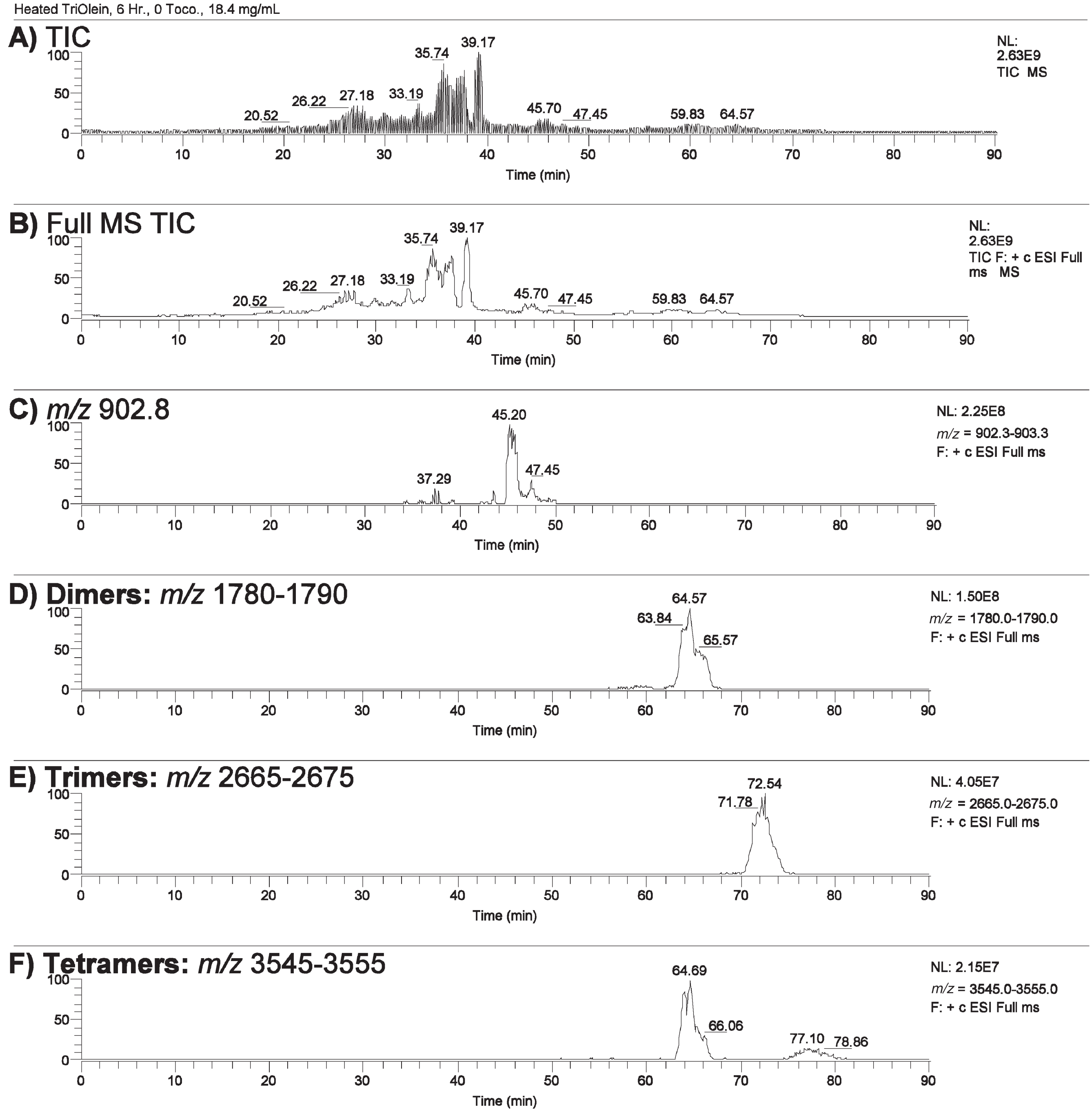

FIG. 1. Total ion chromatograms (TIC) and extracted ion chromatograms of triolein and high M.W. (HMW) TAG oxidation product (TAGOX) oligomers. ESI, electrospray ionization.

expanded view of the base peak mass range given in the right side panel. The large number of carbon atoms on such dimers (= 114), each having a 1.1% probability of being a ^{13}C isotope, meant that the *m/z* of the 1 × ^{13}C-bearing isotope variant was the base peak in many dimer mass spectra. These types of dimers have been discussed previously, as they were observed under APCI–MS (18) and ESI–MS (19) conditions. The *m/z* values 1783.5/1784.5 arose from the dimer that lost two additional hydrogens during dimerization. A mass spectrum showing the *m/z* values 1783.5/1784.5 as the base peak is shown in Figure 2A. The last portion of the dimer peak in Figure 1D contained dimers having *m/z* of 1787.5/1788.5, as we previously mentioned (19). These were triolein molecules joined with no net loss of hydrogens. The chromatographic separation that we previously used allowed only molecules up to the sizes of dimers to elute. We modified the chromatographic system to elute dimers earlier and changed the mass spectral acquisition program to allow detection of higher masses.

Carbon-linked trimers. Figure 1E is a chromatogram extracted from the TIC, showing the masses corresponding to

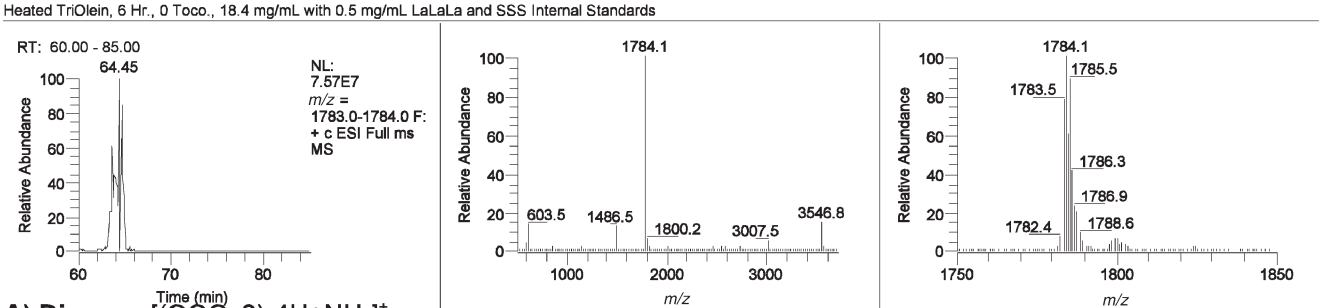

A) Dimers : [(OOOx2)-4H+NH$_4$]$^+$

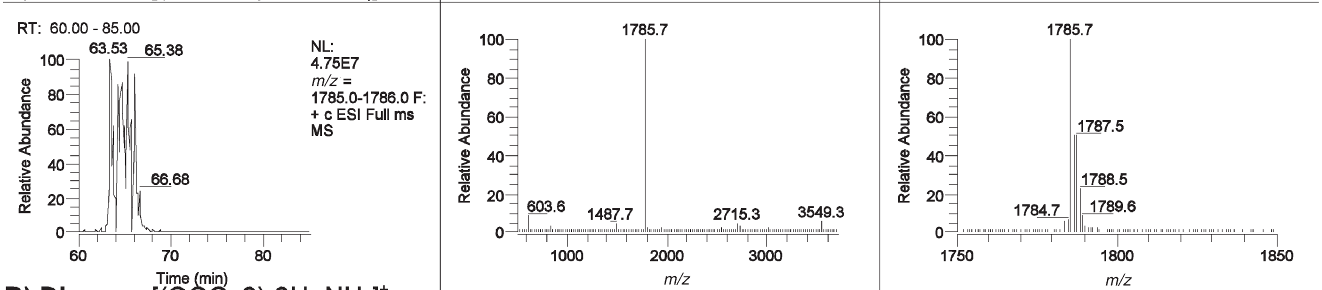

B) Dimers : [(OOOx2)-2H+NH$_4$]$^+$

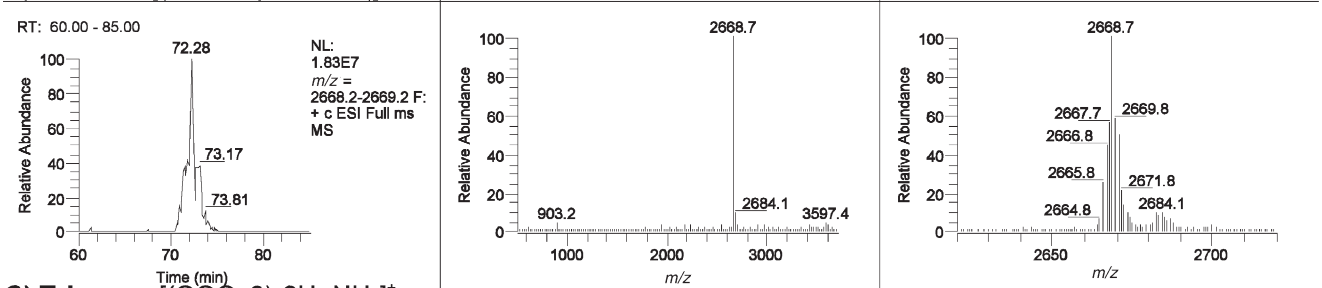

C) Trimers : [(OOOx3)-6H+NH$_4$]$^+$

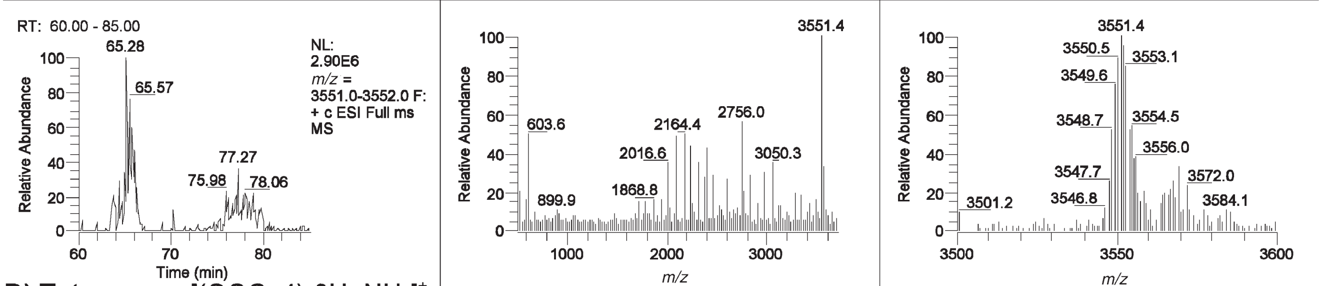

D) Tetramers : [(OOOx4)-8H+NH$_4$]$^+$

FIG. 2. Extracted ion chromatograms, and ESI–MS mass spectra of HMW TAGOX oligomer ammonium adducts. OOO, triolein; SSS, tristearin; LaLaLa, trilaurin; see Figure 1 for other abbreviations.

trimers, formed by joining three intact triolein molecules. Figure 2C shows the mass spectrum averaged across the time region 70.9–73.8 min in Figure 1E. The base peak at *m/z* 2668.7 in the mass spectrum in Figure 2C showed the formation of trimers with the loss of four or six hydrogens. Trimers contain 171 carbon atoms, so the 1 × ^{13}C isotopic variants were the base peaks in mass spectra of trimers, with large peaks also from the 2 × ^{13}C variants, having abundances greater than 96%. For instance, the monoisotopic mass of the trimer formed by joining together three triolein molecules, with a loss of four hydrogens (one at each carbon involved in the C–C bonds) was 3 × 884.78 (= 2654.4) – 4 H + NH$_4$ = 2668.3 amu. But since the trimer contained 171 carbons (as well as 310 hydrogens, etc.), the normalized calculated isotopic abundances of the 2668.3/**2669.3**/2670.3/2671.3/2672.3 peaks are 52.4/**100.0**/96.8/63.3/31.5%, respectively (calculated using a freely available M.W. and isotopic abundance calculator program, Molecular Weight Calculator, v. 6.22) (most abundant isotope in bold). The calculated monoisotopic mass of the trimer formed by three triolein molecules with a loss of six hydrogens, or "trimer – 6H," was 2666.3 amu. The calculated isotopic abundances of the 2666.3/**2667.3**/2668.3/2669.3/2670.3 peaks would be 52.5/**100.0**/96.7/63.3/31.5%, respectively. When both types of trimers are present simultaneously, the net mass spectrum would result from an admixture of the above isotopic abundances, in the relative proportions in which the two species are present. When the "trimer – 6H" is present in an amount between 1.5 and 16 times the amount of the "trimer – 4H" species, the resultant mass spectrum would have a base peak of 2668.3 (based on a normalized ratio-weighted average of the foregoing isotopic abundances, calculated using a Microsoft Excel spreadsheet). Thus, the peak series in the right panel of Figure 2C exhibited a *m/z* 2668.7 base peak that occurred as a combination of the [trimer – 4 H + NH_4]$^+$ and the [trimer (with 2 × ^{13}C) – 6 H + NH_4]$^+$ molecules.

Carbon-linked tetramers. Figure 1F and Figure 2D show ESI–MS EIC and mass spectra of ammonium adducts of intact triolein tetramers. It is noteworthy that such large neutral molecules containing no additional oxygen functional groups were capable of forming substantial abundances of ionized molecules with the ammonium formate sheath liquid solution. In Figure 1F, tetramers are also seen that were formed from dimers in the ESI source. The dimers that were formed during the heated oxidation process were chromatographically resolved and eluted at longer retention times than the dimers and trimers. The tetramers that were formed in the ESI source from dimers occurred at the same chromatographic retention time as the dimers that gave rise to them. Figure 2D shows the mass spectrum of the intact, chromatographically resolved tetramer ammonium adducts. The background spectrum rose substantially at the end of the chromatographic run, when the proportion of methylene chloride went to 75% composition. This gave rise to a series of polymeric peaks having an average repeating unit of 74 amu and reduced the signal-to-noise ratio in the mass spectra. Nevertheless, the intact tetramer ammoniated molecular ion was clearly visible in the mass spectra and produced a distinguishable peak in the EIC.

As expected from the discussion of trimers above, the contribution from the ^{13}C isotopic peaks in the tetramers was even more pronounced than in the case of trimers. The ammoniated tetramer with no additional sites of unsaturation had a monoisotopic mass of 884.78 × 4 (=3539.2) – 6 H + NH_4 = 3551.1 amu. The loss of 6 H assumes loss of one hydrogen at each carbon involved in the three linkages necessary to join four triolein molecules. The peaks produced by such a tetramer would be 3551.1/3552.1/**3553.1**/3554.1/3555.1/3556.1 amu, with isotopic abundances of 30.6/77.8/**100.0**/86.6/56.8/30.1%, respectively. One can see from the calculation of isotopic abundances that tetramers are expected to give molecules with 2 × ^{13}C isotopes as base peaks. As with trimers, some tetramers were formed that had additional sites of unsaturation. The tetramer formed as the "tetramer – 8 H" (having one more site of unsaturation than the pure triolein tetramer minus the six linkage hydrogens) had calculated masses of 3549.1/3550.1/**3551.1**/3552.1/3553.1/3554.1 amu, and with isotopic abundances of 30.6/77.9/**100.0**/86.6/56.8/30.1%, respectively. Such large molecules were also found to lose two more hydrogens to form masses of 3547.1/3548.1/**3549.1**/3550.1/3551.1/3552.1, having isotopic abundances of 30.7/77.9/**100.0**/86.7/56.7/30.1%, respectively. These three possible tetramers occurred chromatographically overlapped and gave rise to a set of peaks in the range 3547 to 3556, as seen in Figure 2D. The peaks 3547/3548/3549/3550/3551/3552/3553/3554 would occur in varying isotopic intensities, based on the amount of each tetramer molecular species. The isotopic abundances that appear in mass spectra would be the normalized percent-weighted average of an admixture of the isotopic percentages given above for each tetramer (normalized to 100% for the base peak). When the above isotopic distributions for the tetramers were combined in different proportions in a Microsoft Excel spreadsheet, it was found that any level of the "tetramer – 8 H" molecule at or higher than 1:**1.6**:1 for the "tetramer – 10 H"/"tetramer – 8 H"/tetramer – 6 H" molecules resulted in a *m/z* 3551 base peak. The *m/z* 3551 base peak also resulted from the ratio of the "tetramer – 10 H" between 1.3:1:1 and 1.7:1:1. It may be possible to compare the isotope ratios of the peaks observed in spectra such as that in Figure 2D to the theoretical isotope ratio calculated as a normalized percent-weighted average of the isotopic abundances given above to calculate the most likely composition of the three tetramer molecules. As a first approximation, the ratio of -10H/-8H/-6H that produced the least average absolute error between the calculated isotope ratios of masses from 3547 to 3555, and which had *m/z* 3551 as a base peak, was the ratio 3:2.4:2.3. In this ratio, the calculated isotopic ratios for the masses 3547/3548/3549/3550/**3551**/3552/3553/3554/3555 were 19.1/48.58/77.69/92.87/**100.0**/99.22/84.56/59.67/34.97%, respectively, compared with the observed abundances of 24.9/51.4/74.6/89.2/**100.0**/95.62/84.9/51.8/36.3%. The ratio of 3:2.4:2.3 (or 30:24:23) for the -10H/-8H/-6H molecular species produced an average absolute error of 3.2%, between the calculated ratio-weighted normalized isotopic abundances and those observed in the mass spectrum in Figure 2D. The use of isotope abundances to obtain estimates of the ratios of molecular species requires further investigation.

MS and MS/MS mass spectra of oxygen-containing and carbon-linked oligomers. In a way analogous to the oxygen-containing dimers that we previously reported (17,19), trimers and tetramers also occurred with additional oxygen-containing functional groups having one, two, or three additional oxygens. These were more polar and eluted with shorter retention times than simple trimers or tetramers. Figure 3 shows the EIC of the mass ranges of dimers and oxidized dimers, trimers and oxidized trimers, and tetramers and oxidized tetramers. Comparison of Figure 3 with Figure 1 shows that the pure oligomers without additional oxygens eluted with peak maxima at 64.57, 72.54, and 77.10 min for the dimers, trimers, and tetramers, respectively. In Figure 3, peaks can be seen to elute before these retention times. These earlier eluted peaks represented dimers, trimers, and tetramers containing additional oxygen atoms. These oxygen atoms may occur as a bridging oxygen or may occur as oxygen functional groups on the carbon-linked oligomers. In the full population of molecules, both classes were expected to be present. The mass spectra in Figures 3D–F are the average mass spectra across both the oxygen-containing and normal oligomer peaks. The expanded view of the ammoniated molecule mass region is seen in the right panels of Figures 3D–F.

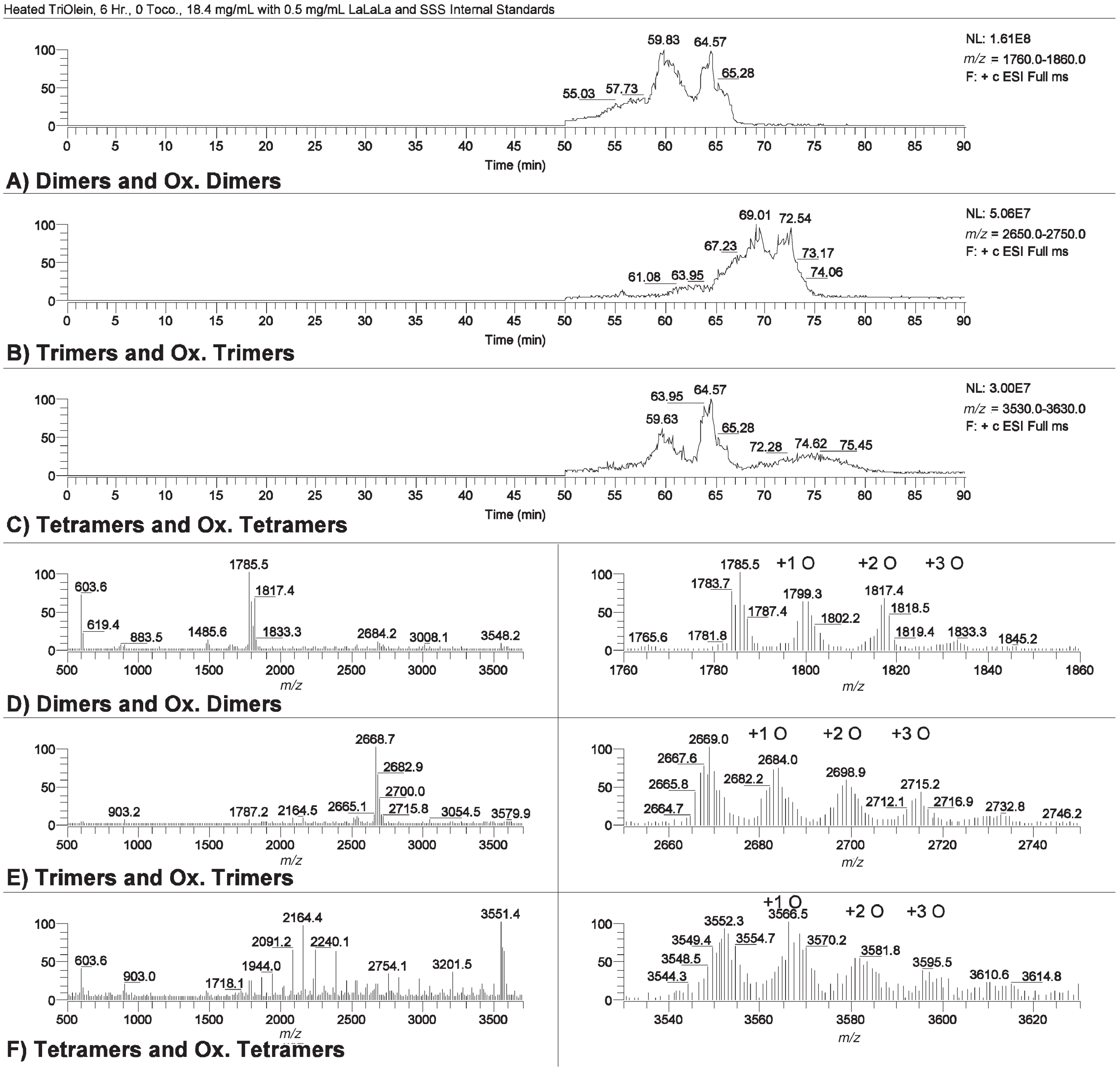

FIG. 3. Extracted ion chromatograms (A–C) and ESI–MS mass spectra (D–F) of HMW TAGOX. Right panels of D–F show the mass spectra with expanded scales. Labels above peak clusters indicate the number of additional oxygen atoms associated with each oligomer *m/z* range. HMW TAGOX containing oxo-groups eluted before oligomers without additional oxygens (compare to Fig. 1). See Figures 1 and 2 for abbreviations.

These regions show the oxygen-containing oligomer *m/z* values. Peaks can be seen for molecules containing one, two, or three additional oxygen atoms, and each of these may have one or two additional sites of unsaturation, as already discussed. Work is underway to prepare a full report demonstrating quantitative analysis of all oligomeric and oxidized oligomeric species, compared with added internal standard, in samples containing varying levels of antioxidant, added to lessen formation of the HMW TAGOX.

We also obtained MS/MS and some MS/MS/MS data from the ammoniated oligomeric molecules. Figure 4 presents MS, MS^2, and MS^3 spectra of normal and oxygen-containing oligomers. The MS^n spectra are averaged across all MS^n spectra obtained from a given precursor ion. The full-scan mass spectrum in Figure 4A shows a base peak at *m/z* 1800.3 arising from a dimer having one additional oxygen atom and one additional site of unsaturation. The monoisotopic weight of the intact ammoniated molecule was 1799.6, and the isotopic distribution was 1799.6/**1800.6**/1801.6/1802.6 = 78.6/**100.0**/65.2/29.0%. This was not completely chromatographically resolved from the molecule containing two oxygens, so a peak arising from *m/z* 1816.7 also can be seen. The MS/MS spectrum of the 1800.3 precursor is seen in the middle panel. The base peak in the MS/MS spectrum was the [M – RCOO]$^+$

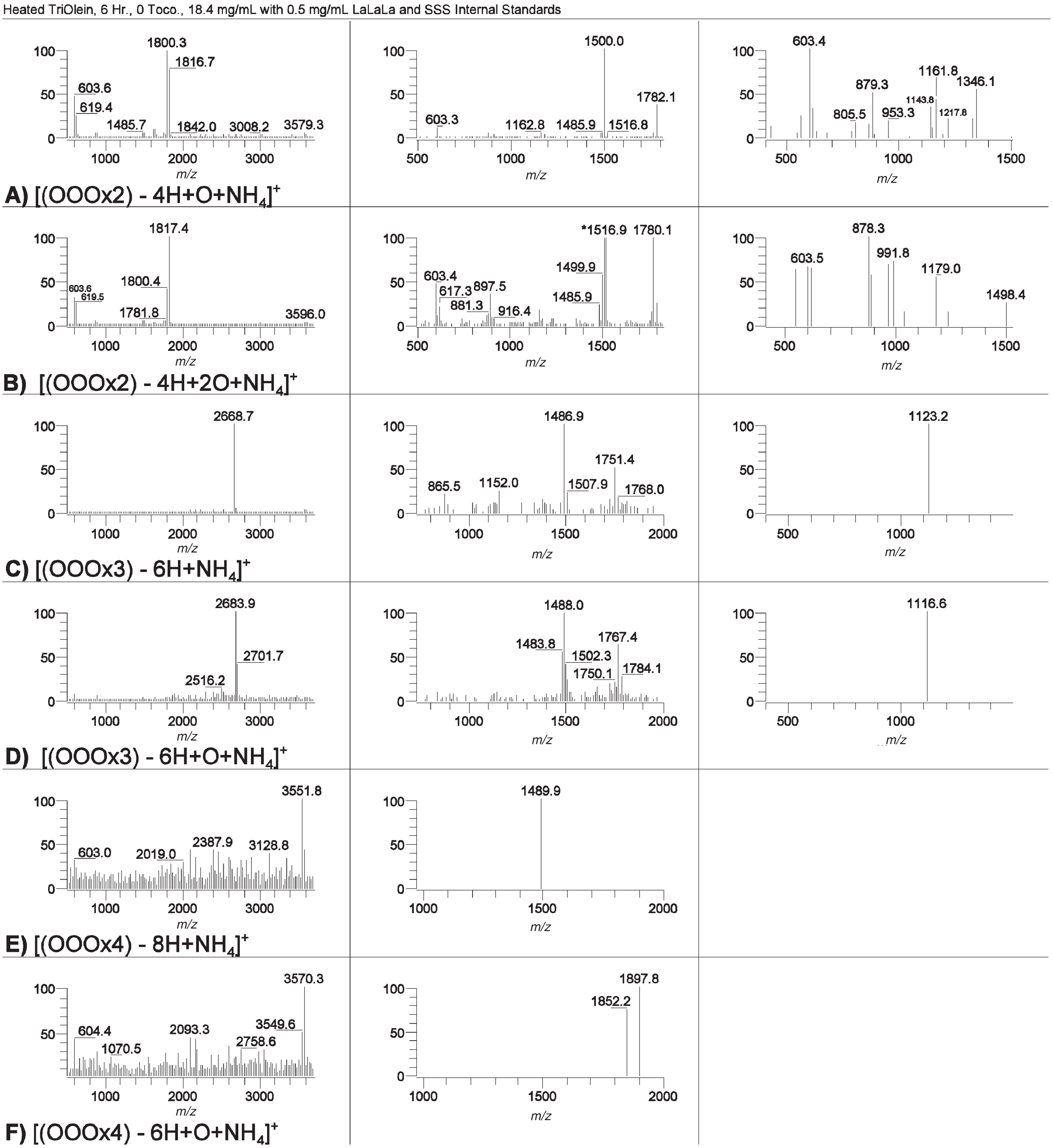

FIG. 4. ESI–MS (first column), MS/MS (second column), and MS/MS/MS (third column) mass spectra of HMW TAGOX with and without additional oxygen functional groups. (A) Dimer + 1 O, (B) Dimer + 2 O, (C) Trimer, (D) Trimer + 1 O, (E) Tetramer, (F) Tetramer + 1 O. Triolein (OOO) has an isotopic mass of 884.8. Oligomers contain multiple ^{13}C. See Figure 1 for abbreviations.

fragment (M = 1781.6). In the MS^3 spectrum in the right panel of Figure 4A, we found some peaks that were readily identifiable, such as the peak at *m/z* 1217.8 corresponding to the [M – RCOO – RCOOH]$^+$; the *m/z* 603.4 = the dioleoyl DAG fragment ion, [DAG]$^+$ = [OO]$^+$; the *m/z* 617.5 = the epoxy-dioleoyl DAG fragment,

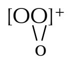

(where "O" is oleoyl and "o" is oxygen), and the *m/z* 879.3 that is equivalent to [OLLn]$^+$ formed by cleavage of the linkage and loss of the oxygen. Other peaks in the MS^3 mass spectrum require more explanation and elucidation of mechanism schemes than is appropriate for this first report.

The mass spectrum in the first panel of Figure 4B showed a base peak of 1817.4. This was produced by the mixture of the isotopic distributions of at least two dimer molecules containing two additional oxygen atoms. The molecule $[(\mathrm{OOO} \times 2) - 4\mathrm{H} + 2\mathrm{O} + \mathrm{NH}_4]^+$ had isotopic masses of 1815.6/**1816.6**/1817.6/1818.6 having abundances of 78.5/**100.0**/65.4/29.2%, whereas $[(\mathrm{OOO} \times 2) - 2\mathrm{H} + 2\mathrm{O} + \mathrm{NH}_4]^+$ had isotopic masses of 1817.6/**1818.6**/1819.6/1820.6 with the same isotopic abundances of 78.5/**100.0**/65.4/29.2%. These two molecular species were not chromatographically resolved. The combination of these two species produced a mass spectrum having a *m/z* 1817.4 base peak in Figure 4B. According to the calculated isotopic abundances above, any combination of the two species in a ratio of equal to or less than 2.2:1 would give a 1817 base peak, as would any ratio equal to or greater than 1:1.6. Thus, at least two molecular species contributed to the *m/z* 1817 peak. The $[(\mathrm{OOO} \times 2) - 4\mathrm{H} + 2\mathrm{O} + \mathrm{NH}_4]^+$ and $[(\mathrm{OOO} \times 2) - 2\mathrm{H} + 2\mathrm{O} + \mathrm{NH}_4]^+$ molecules could, of course, take a variety of forms including a dimer linked by an oxygen with an epoxide either across a double bond (to form an epoxystearate) or not across a double bond (an epoxy oleate), or a carbon-linked dimer with a hydroperoxide group on a fatty acyl chain, or an oxygen-linked dimer with a hydroxy group, etc. The full-scan MS spectrum and the MS/MS spectrum provided clues to the identities of these oxidized dimers. In the full-scan mass spectrum, peaks appear at 601.5 (16.2%), 603.6 (30.3%), 617.4 (3.2%), and 619.5 (25.2%). The *m/z* 619.5 peak was especially revealing, because it corresponded to an epoxy-stearoyloleoyl DAG fragment,

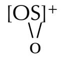
$$[\mathrm{O}\underset{\mathrm{O}}{\underset{\backslash/}{\mathrm{S}}}]^+$$

The 601.5 peak resulted from the loss of the epoxy group to form the fatty chain with two sites of unsaturation, as we previously demonstrated using APCI–MS (16). The ratio of 619.5/601.5 in the spectrum of the dimer was 1.56/1; the ratio of 619.5/601.5 in the spectrum of

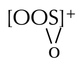
$$[\mathrm{OO}\underset{\mathrm{O}}{\underset{\backslash/}{\mathrm{S}}}]^+$$

eluted at 39.17 min in this sample (spectrum not shown here, see peak in Fig. 1B) was 1.53/1. The peak at *m/z* 617.5 indicated the presence of epoxy-dioleyl DAG,

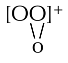
$$[\mathrm{O}\underset{\mathrm{O}}{\underset{\backslash/}{\mathrm{O}}}]^+$$

as well. The MS/MS spectrum in the middle panel of Figure 4B gave two peaks at *m/z* 1798.2 (25.91%) and *m/z* 1800.0 (23.5%), corresponding to the protonated molecules of these two oxygen-linked epoxy-containing dimers,

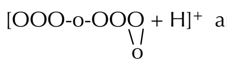
$$[\mathrm{OOO\text{-}o\text{-}OO}\underset{\mathrm{O}}{\underset{\backslash/}{\mathrm{O}}} + \mathrm{H}]^+$$

and

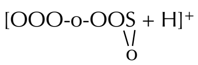
$$[\mathrm{OOO\text{-}o\text{-}OO}\underset{\mathrm{O}}{\underset{\backslash/}{\mathrm{S}}} + \mathrm{H}]^+$$

Fragment ions, and their calculated masses, that would result from the epoxide-containing oxygen-linked dimers already discussed are shown in Scheme 1.

Figure 4C shows the MS, MS^2, and MS^3 spectra of the ammonium adduct of the carbon-linked trimer formed without additional oxygen atoms, but having one additional site of unsaturation, $[(\mathrm{OOO} \times 3) - 6\mathrm{H} + \mathrm{NH}_4]^+$. The *m/z* 1486.9 base peak arose from the fragment that was equivalent to a carbon-linked dimer minus one fatty acyl chain, $[(\mathrm{OOO} \times 2) - 2\mathrm{H}\text{-}\mathrm{RCOO}]^+$, $\mathrm{C}_{96}\mathrm{H}_{173}\mathrm{O}_{10}$. This fragment provided further evidence for the absence of additional oxygen atoms. On the other hand, Figure 4D shows the trimer formed with the addition of one oxygen atom. As with the dimers, several possible structures could contain one oxygen atom. However, given the high levels of epoxides known to be present, as seen in Figure 1 at 37.65 min and 39.17 min, the carbon-linked trimers with an epoxide group on one of the fatty chains were expected to predominate. The two types of epoxides, not across a double bond, $[(\mathrm{OOO} \times 3) - 6\mathrm{H} + \mathrm{O} + \mathrm{NH}_4]^+$ (FM = 2682.33), or across a double bond, $[(\mathrm{OOO} \times 3) - 4\mathrm{H} + \mathrm{O} + \mathrm{NH}_4]^+$ (FM = 2684.35), led to overlapping isotopic masses having a net base peak at 2683.9. However, based on the isotopic pattern, and specifically the presence of a substantial peak at 2681.1, there was another species that contributed to the isotopic pattern, which was a molecule having an epoxide not across a double bond, plus one additional site of unsaturation, $[(\mathrm{OOO} \times 3) - 8\mathrm{H} + \mathrm{O} + \mathrm{NH}_4]^+$ (FM = 2680.32). Together, these species had the following isotopic masses and abundances (in order from least mass to highest): 2680.3 (52.5)/**2681.3(100.0)**/2682.3(96.9)/2683.3(63.5)/2684.3(31.7)/2685.3(12.8)/2686.3(4.4)/2682.3(52.4)/**2683.3(100.0)**/2684.3(96.9)/2685.3(63.5)/2686.3(31.7)/2687.3(12.8);2684.3 (52.4)/**2685.3(100.0)**/2686.3(96.9)/2687.3(63.5)/2688.3(31.7)/2689(12.8%).

The linear combination of these three isotopic patterns revealed that any combination in which the -8H/-6H/-4H were present in a ratio of 1:6.6:1 or higher -6H resulted in a 2683.3 base peak. The 2680.3 species could be at a level as high as 9.4:6.6:1 and still produce a *m/z* 2683.3 base peak. If the 2680.3 species were present at a relative ratio of 9.4:x:1, the 2682.3 species, "x," could be any value above 6.6 and still yield a 2683.3 base peak. The whole number ratio that produced the least absolute error between the observed isotopic abundances and the calculated combination of abundances was 75:81:1, for the -8H/-6H/-4H. In the MS/MS spectrum in Figure 4D, the envelope of peaks at between 1483.8 and 1488.0 corresponds to $[(\mathrm{OOO} \times 2) - n\mathrm{H} - \mathrm{RCOO}]^+$ fragments containing no additional oxygens, where "*n*" is 2 or 4 hydrogens. This reflects a carbon-linked fragment from the trimer. The peak at *m/z* 1502 was the $[(\mathrm{OOO} \times 2) - 2\mathrm{H} - \mathrm{RCOO} + \mathrm{O}]^+$ fragment, where the additional oxygen was across a double bond, to give an

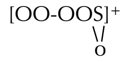
$$[\mathrm{OO\text{-}OO}\underset{\mathrm{O}}{\underset{\backslash/}{\mathrm{S}}}]^+$$

($\mathrm{C}_{96}\mathrm{H}_{173}\mathrm{O}_{11}{}^+$) fragment. The *m/z* 1502.3 peak reflected the presence of one additional oxygen in this fragment. One

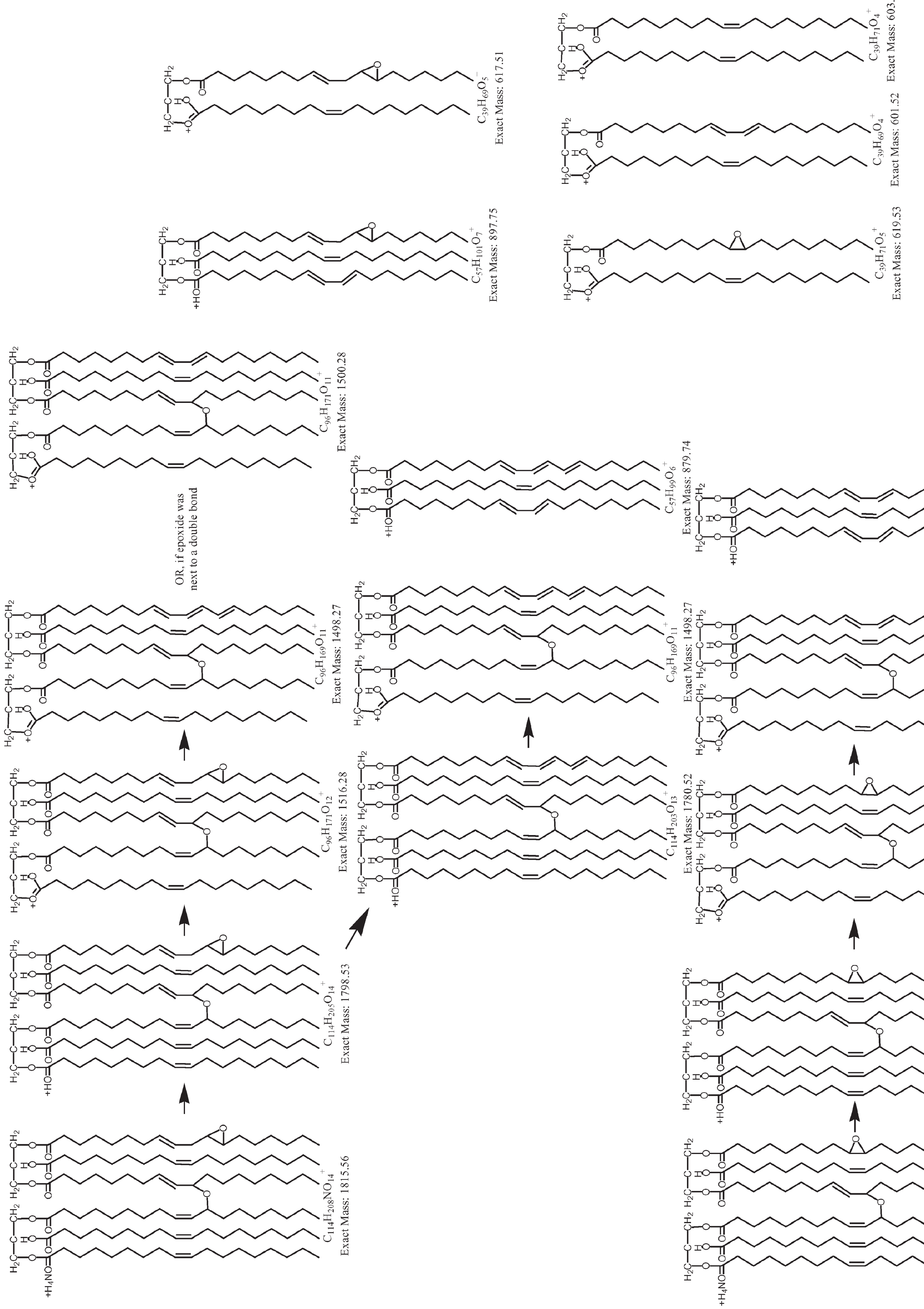
+H4NO
H2C
CH2
C114H208NO14+
Exact Mass: 1815.56
+HO
C114H205O14+
Exact Mass: 1798.53
C96H171O12+
Exact Mass: 1516.28
C96H169O11+
Exact Mass: 1498.27
OR, if epoxide was next to a double bond
C96H171O11+
Exact Mass: 1500.28
C57H101O7+
Exact Mass: 897.75
C39H69O5+
Exact Mass: 617.51
C114H203O13+
Exact Mass: 1780.52
C96H169O11+
Exact Mass: 1498.27
C57H99O6+
Exact Mass: 879.74
C114H210NO14+
Exact Mass: 1817.58
C114H207O14+
Exact Mass: 1800.55
C96H173O12+
Exact Mass: 1518.29
C96H171O11+
Exact Mass: 1500.28
C57H101O6+
Exact Mass: 881.76
C39H71O5+
Exact Mass: 619.53
C39H69O4+
Exact Mass: 601.52
C39H71O4+
Exact Mass: 603.54

SCHEME 1

shortcoming of the current MS/MS data was that the daughter ion *m/z* range did not go up to the mass of the ammoniated molecule, and the low mass in the scan range did not go down to the DAG fragment ion *m/z* values, presumably because of the "q" factor used for the MS/MS experiment. Further analysis will be necessary to optimize the "q" factor to extend the range of MS/MS masses. Because the low-mass range was not low enough to detect the DAG fragment ions, we cannot exclude the possibility that the $[(\text{OOO} \times 3) - 6\text{H} + \text{O} + \text{NH}_4]^+$ arose from the trimer containing one carbon-linkage between trioleins and one oxygen-linkage between trioleins, instead of carbon-linked trioleins plus one epoxide group. As can be seen from the remainder of Figure 4, larger oligomers gave poorer MS/MS spectra due to the lower population of precursor ions. MS^3 spectra of tetramers were not observed.

Dimerization of tristearin. Based on the dimerization of triolein with no loss of hydrogens or with loss of two or four hydrogens, we believed that even tristearin, with no sites of unsaturation, might form dimers under heated oxidation conditions. We found that not only dimers but also a full range of oxidation products were formed. Figure 5 shows the total ion chromatogram and several extracted ion chromatograms

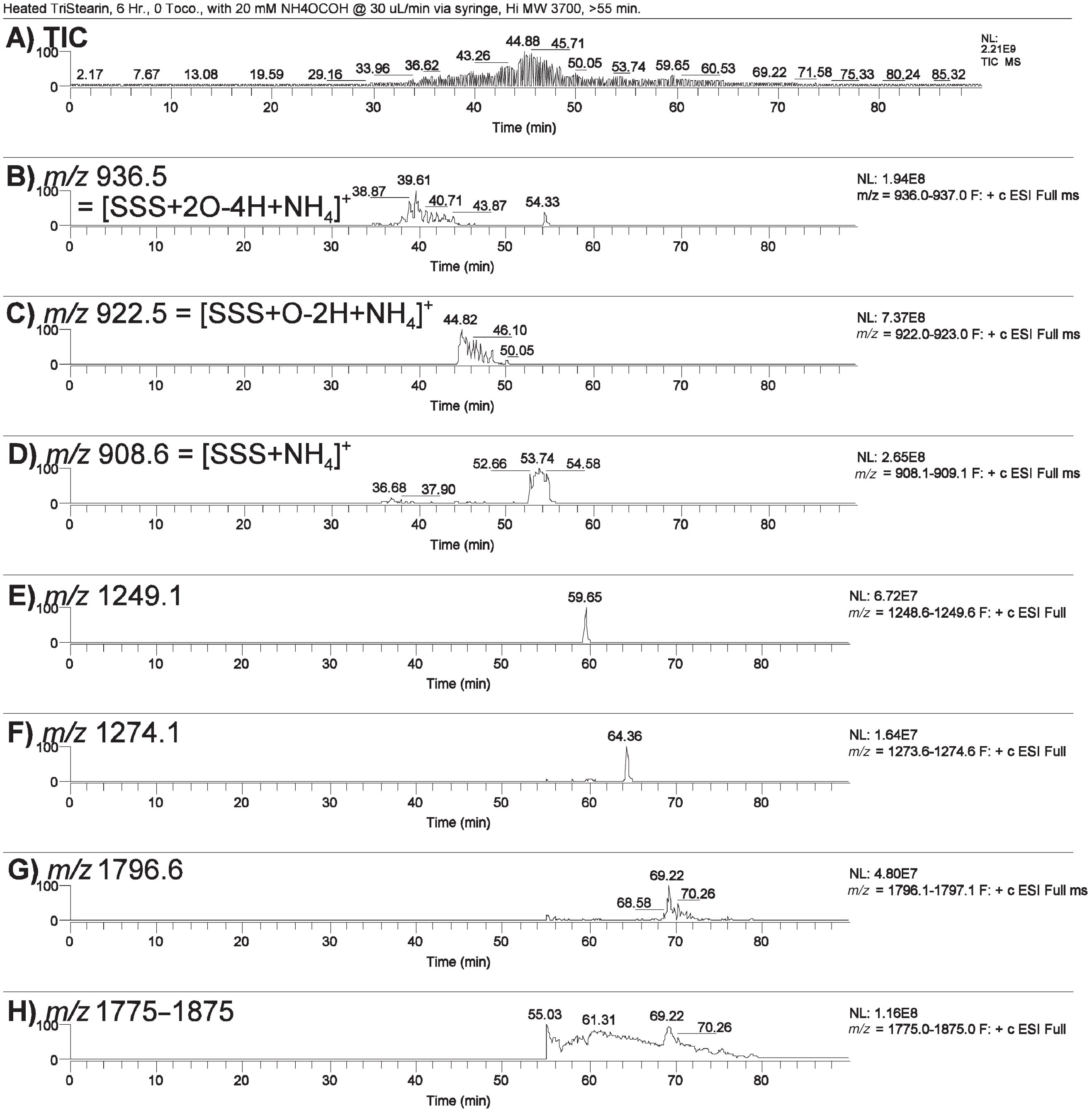

FIG. 5. TIC and extracted ion chromatograms of SSS and SSS oxidation products. See Figures 1 and 2 for abbreviations.

of ammonium adducts of tristearin ($[M + NH_4]^+ = 908.9$ amu) and tristearin oxidation products. Figure 5B shows an EIC of *m/z* 936.5, representing ammonium adducts of tristearin oxidation products containing two oxygen atoms and loss of four hydrogens, $[SSS + 2O - 4H + NH_4]^+$. The mass spectrum in Figure 6A is an average spectrum across this peak and exhibits a DAG fragment ion at *m/z* 635.4 that also reflects the addition of two oxygens and loss of four hydrogens, compared with the normal distearoyl DAG fragment at *m/z* 607.5. The loss of four hydrogens, instead of two, would argue for the molecule to be a diepoxide, rather than either an epidioxide, which would only lose two hydrogens, or a hydroperoxide, which would exhibit no net loss of hydrogens. Other peaks arising from chain-shortened TAGOX, of the type we previously reported (17,19), are also present in the mass spectrum, as they eluted in the same time region. Figure 5C is an EIC of *m/z* 922.5, which is the ammonium adduct of a tristearin molecule containing one oxygen, with the loss of two

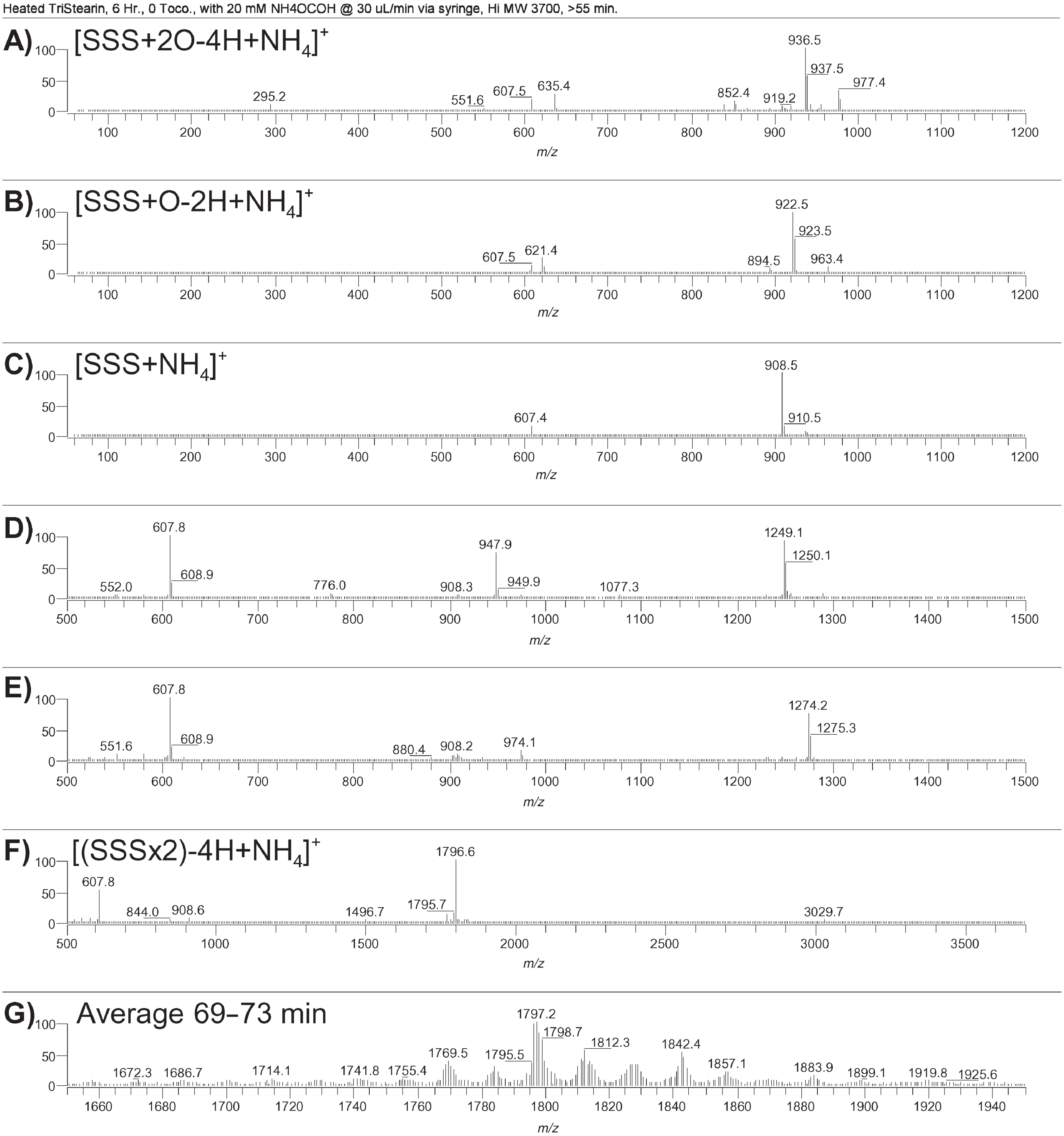

FIG. 6. ESI–MS mass spectra of SSS and SSS oxidation products. Spectra are averaged across peaks B through H in Figure 5. For abbreviations see Figures 1 and 2.

hydrogens, such as an epoxy-tristearin molecule. The mass spectrum in Figure 6B shows the average mass spectrum across this peak and exhibits an ammonium adduct base peak at *m/z* 922.5, and a DAG fragment ion peak at *m/z* 621.4 that confirmed the addition of the oxygen with loss of two hydrogens for the epoxy-stearoyl DAG fragment ion. The MS of the normal tristearin ammonium adduct is seen in Figure 6C.

The dimer formed by the union of two tristearin molecules is shown in the EIC in Figure 5G, and the mass spectrum is shown in Figure 6F. These data clearly show that tristearin did produce intact dimers that were chromatographically separable. The masses of the dimers indicated that they formed with the loss of two or four hydrogens, similar to the behavior of triolein. The EIC in Figure 5H shows the mass range associated with all tristearin dimers, including those with additional oxygen atoms. There is a broad peak containing a variety of oxygenated dimers that eluted prior to the dimer without additional oxygens. An average mass spectrum across this broad peak is shown in Figure 6G, to demonstrate the variety of species present.

We also wish to mention the presence of chain-addition products of tristearin, analogous to those we reported previously for triolein (17,19). Figure 5E shows an EIC of *m/z* 1249.1 that has a mass consistent with a tristearin molecule plus a MAG fragment, SSS + $RCOOC_3H_6OH$, that lost two hydrogens at the site of union. This had a calculated mass of 890.8 + (283.3 + 59) + NH_4 – 2 H = 1249.1. The *m/z* 1249.1 was the most abundant peak in the mass spectrum in Figure 6D. Another chain-addition product had a *m/z* of 1274.1 and eluted at 64.4 min as shown in Figures 5F and 6E.

Finally, we also report the chain-shortened products formed by cleavage of oxidized tristearin. Figure 7 shows EIC of the ammonium adducts of chain-shortened products having masses starting at 810.4, and increasing in units of 14 Da (CH_2). Also, EIC of the chain-shortened DAG fragment ions from each of the species are shown in the right panel. In each of these chromatograms, two primary sets of peaks were seen, a large pair of peaks that eluted before a single peak that eluted later. As we previously observed (19), there are three primary possibilities for the identities of these peaks. The first likely class of molecules is core aldehydes, produced by cleavage of a fatty acyl chain at a site of oxidation, leaving the oxygen on the chain as an aldehyde. Alternatively, the oxygen could be left behind as an epoxide. These two classes could not be distinguished by mass. One approach to identification of core aldehydes has been demonstrated by Sjovall and co-workers (20,21). It will be possible to perform the separation on the unreacted oxidation products mixture and on the reacted product mixture to identify which peaks disappear from the chromatogram of the unreacted mixture and appear at different retention times in the reacted mixture. The peaks that change positions will be the core aldehydes that reacted to form DNPH derivatives. In fact, both core aldehydes and epoxides may be present. There are peaks that appeared at shorter retention times than the largest peaks in the EIC in Figure 7. If all three classes (aldehydes, epoxides, and non-oxo acyl chains) were present, the aldehydes would elute first, the epoxy-containing TAG would elute second, and the nonpolar chain-shortened TAG would elute last. Since small sets of peaks were eluted before the largest peaks, this order would tend to argue for the largest peaks being epoxy-containing species, with the smaller preceding peaks being core aldehydes. However, we are not yet in a position to make an unambiguous identification of these species without first performing the DNPH derivatization experiments.

Based on the relative sizes of the epoxide or core aldehyde peaks, it was apparent that the *sn*-2 peak eluted before the *sn*-1,3 peak. From statistical considerations, the *sn*-1,3 isomers are present in a combined amount twice that of the *sn*-2 isomer. The peaks in Figure 7 clearly showed one peak that was smaller, preceding a larger peak of approximately twice the size of the earlier peak. This would indicate that the *sn*-2 isomer eluted before the *sn*-1,3 isomers. This is in complete agreement with the discussion by Sjovall *et al.* (20), in which they reported that the 2-isomer eluted ahead of the 1,3-isomers for aldehydes and hydroperoxy species, although the elution factors tabulated and pictured for the 2-isomers (20) were longer than the elution factors for the corresponding 1,3-isomers.

The other class of molecules that was isobaric with the oxo-acyl chain-containing TAG was the class formed by cleavage of the oxidized chain, with the oxygen functional group being lost with the leaving fragment. These form chain-shortened acyl chains with no additional oxygen functional group. A neutral carbon chain was isobaric with the polar carbon chain containing one less carbon atom. For instance, the core aldehyde SS,$C_{10}H_{17}O_3$ was isobaric with SS,$C_{11}H_{21}O_2$, each having a calculated mass of 810.7x Da. But, of course, these two classes were chromatographically separated, with the longer, non-oxo chain eluted later. Regioisomers of these species were not chromatographically separated, and they eluted as one peak.

The peak at *m/z* 810.4, as mentioned above, corresponded to both $[SS,C_{10}H_{17}O_3 + NH_4]^+$ (= 10-oxo) and $[SS,C_{11}H_{21}O_2 + NH_4]^+$. The peak at 824.5 corresponded to ammonium adducts of both SS,$C_{11}H_{19}O_3$ (= 11-oxo) and SS,$C_{12}H_{23}O_2$; the peak at *m/z* 838.5 corresponded to adducts of both SS,$C_{12}H_{21}O_3$ (= 12-oxo) and SS,$C_{13}H_{25}O_2$; etc. up to *m/z* 894.5, which corresponded to ammonium adducts of both SS,$C_{16}H_{29}O_3$ (= 16-oxo) and SS,$C_{17}H_{33}O_2$. In all cases for oxo-containing and completely nonpolar chain-shortened species, the DAG fragment ion in the right panel of Figure 7 confirmed the identification made based on the intact ammoniated molecule. Although EIC of 10-oxo to 16-oxo species are shown in Figure 7, chain-shortened species down to 4-oxo were observed. There was a substantial decrease in the amount of 4-oxo compared with 5-oxo and larger species. DAG fragment ions for every chain-shortened species down to *m/z* 439.2, arising from the 5-oxo species, were observed.

We have reported here ESI–MS chromatograms and spectra of ammonium adducts of intact trimers and tetramers

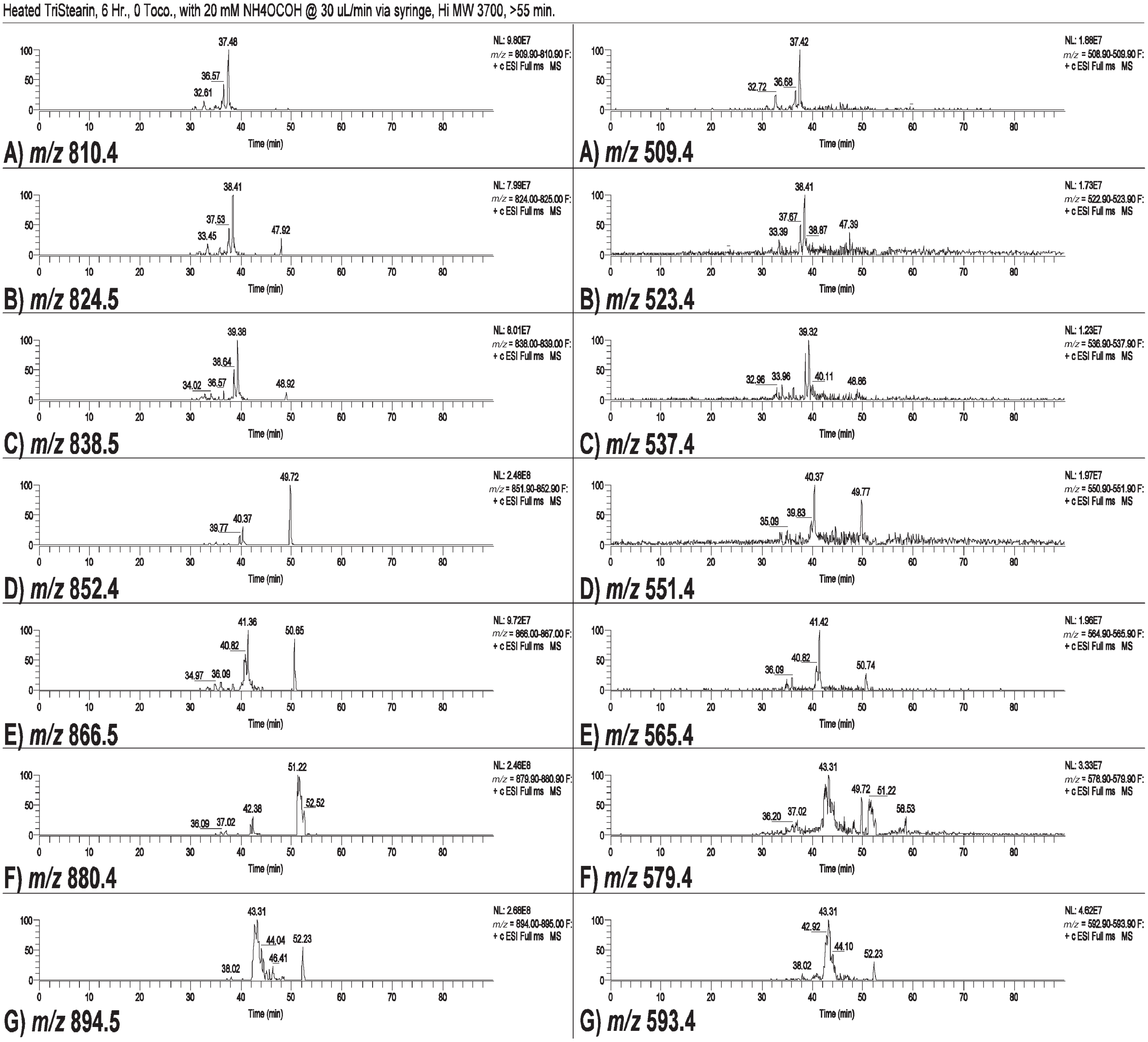

FIG. 7. Extracted ion chromatograms of intact ammonium adducts (left panels) and DAG fragment ions (right panels) of chain-shortened SSS oxidation products (core aldehydes or epoxides, and nonpolar acyl chains). See Figure 2 for abbreviation.

formed from triolein, with and without additional oxygen-containing functional groups, and with and without additional sites of unsaturation. To our knowledge, no previous report has provided direct on-line LC/ESI–MS mass spectral evidence for these large, neutral oligomeric molecules. Quantitative analysis of these species will be reported elsewhere. We also reported the first on-line LC/ESI–MS evidence for the formation of tristearin dimers with and without additional oxygen functional groups, and with and without additional sites of unsaturation. We also reported chain-addition products and a full series of chain-shortened products from the oxidation of tristearin.

REFERENCES

1. Chan, H.W. (ed.) *Autoxidation of Unsaturated Lipids,* Academic Press, London, 1987.
2. Frankel, E.N., Volatile Lipid Oxidation Products, *Prog. Lipid Res. 22*:1–33 (1982).
3. Frankel, E.N., Recent Advances in Lipid Oxidation, *J. Sci. Food Agric. 54*:495–511 (1991).
4. Grosch, W., Reactions of Hydroperoxides—Products of Low Molecular Weight, in *Autoxidation of Unsaturated Lipids,* edited by H.W.S. Chan, Academic Press, London, 1987.
5. Miyashita, K., K. Fujimoto, and T. Kaneda, Formation of Dimers During the Initial Stage of Autoxidation in Methyl Linoleate, *Agric. Biol. Chem. 46*:751–755 (1982).
6. Miyashita, K., K. Fujimoto, and T. Kaneda, Structures of Dimers

Produced from Methyl Linoleate During Initial Stage of Autoxidation, *Ibid. 46*:2293–2297 (1982).

7. Miyashita, K., N. Hara, K. Fujimoto, and T. Kaneda, Dimers Formed in Oxygenated Methyl Linoleate Hydroperoxides, *Lipids 20*:578–587 (1985).
8. Neff, W.E., E.N. Frankel, and K. Miyashita, Autoxidation of Polyunsaturated Triacylglycerols. I. Trilinoleoylglycerol, *Ibid. 25*:33–39 (1990).
9. Frankel, E.N., W.E. Neff, and K. Miyashita, Autoxidation of Polyunsaturated Triacylglycerols. II. Trilinolenoylglycerol, *Ibid. 25*: 40–47 (1990).
10. Miyashita, K., E.N. Frankel, W.E. Neff, and R.A. Awl, Autoxidation of Polyunsaturated Triacylglycerols. III. Synthetic Triacylglycerols Containing Linoleate and Linolenate, *Ibid. 25*:48–53 (1990).
11. Hopia, A., A.M. Lampi, V.I., Piironen, L.E.T. Hyvonen, and P.E. Koivistoinen, Application of High-Performance Size-Exclusion Chromatography to Study the Autoxidation of Unsaturated Triacylglycerols, *J. Am. Oil Chem. Soc. 70*:779–784 (1993).
12. Hopia, A., Analysis of High Molecular Weight Autoxidation Products Using High-Performance Size Exclusion Chromatography: I. Changes During Autoxidation, *Lebensm. Wiss. Technol. 26*:563–567 (1993).
13. Hopia, A., Analysis of High Molecular Weight Autoxidation Products Using High-Performance Size Exclusion Chromatography: II. Changes During Processing, *Ibid. 26*:568–571 (1993).
14. Marquez-Ruiz, G., M. Martin-Polvillo, and M.C. Dobarganes, Quantitation of Oxidized Triglyceride Monomers and Dimers as a Useful Measurement for Early and Advanced Stages of Oxidation, *Grasas Aceites 47*:48–53 (1996).
15. Marquez-Ruiz, G., M.C. Perez-Camino, and M.C. Dobarganes, Combination of Absorption and Size-Exclusion Chromatography for the Determination of Fatty Acid Monomers, Dimers and Polymers, *J. Chromatogr. A 514*:37–44 (1990).
16. Neff., W.E., and W.C. Byrdwell, Characterization of Model Triacylglycerol (triolein, trilinolein, and trilinolenin) Autoxidation Products *via* High-Performance Liquid Chromatography Coupled with Atmospheric Pressure Chemical Ionization Mass Spectrometry, *J. Chromatogr. A 818*:169–186 (1998).
17. Byrdwell, W.C., and W.E. Neff, Autoxidation Products of Normal and Genetically Modified Canola Oil Varieties Determined Using Liquid Chromatography with Mass Spectrometric Detection, *Ibid. 905*:85–102 (2001).
18. Byrdwell, W.C., and W.E. Neff, Non-volatile Products of Triolein Produced at Frying Temperatures Characterized Using Liquid Chromatography with Online Mass Spectrometric Detection, *Ibid. 852*:417–432 (1999).
19. Byrdwell, W.C., and W.E. Neff, Dual Parallel Electrospray Ionization and Atmospheric Pressure Chemical Ionization Mass Spectrometry (MS), MS/MS, and MS/MS/MS for the Analysis of Triacylglycerols and Triacylglycerol Oxidation Products, *Rapid Commun. Mass Spectrom. 16*:300–319 (2002).
20. Sjovall, O., A. Kuksis, L. Marai, and J.J. Myher, Elution Factors of Synthetic Oxotriacylglycerols as an Aid in Identification of Peroxidized Natural Triacylglycerols by Reversed-Phase High-Performance Liquid Chromatography with Electrospray Mass Spectrometry, *Lipids 32*:1211–1218 (1997).
21. Sjovall, O., A. Kuksis, and H. Kallio, Reversed-Phase High-Performance Liquid Chromatographic Separation of *tert*-Butyl Hydroperoxide Oxidation Products of Unsaturated Triacylglycerols, *J. Chromatogr. A 905*:119–132 (2001).

[Received March 18, 2003; accepted August 21, 2003]